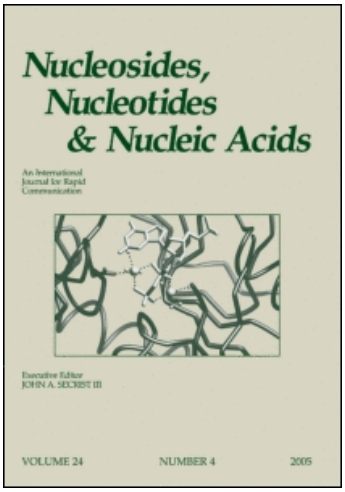

Nucleosides, Nucleotides and Nucleic Acids
Publication details, including instructions for authors and subscription information:
http://www.informaworld.com/smpp/title~content=t713597286

Metalloregulation of Triple Helix Formation by Control of the Loop Conformation

Toshihiro Ihara[ab]; Yoshinobu Sato[a]; Hiroshi Shimada[a]; Akinori Jyo[a]
[a] Department of Applied Chemistry and Biochemistry, Graduate School of Science and Technology, Kumamoto University, Kumamoto, Japan [b] PRESTO, Japan Science and Technology Agency, Saitama, Japan

To cite this Article Ihara, Toshihiro , Sato, Yoshinobu , Shimada, Hiroshi and Jyo, Akinori(2008) 'Metalloregulation of Triple Helix Formation by Control of the Loop Conformation', Nucleosides, Nucleotides and Nucleic Acids, 27: 9, 1084 — 1096
To link to this Article: DOI: 10.1080/15257770802271813
URL: http://dx.doi.org/10.1080/15257770802271813

Nucleosides, Nucleotides and Nucleic Acids, 27:1084–1096, 2008

ISSN: 1525-7770 print / 1532-2335 online
DOI: 10.1080/15257770802271813

Taylor & Francis
Taylor & Francis Group

METALLOREGULATION OF TRIPLE HELIX FORMATION BY CONTROL OF THE LOOP CONFORMATION

Toshihiro Ihara,[1,2] Yoshinobu Sato,[1] Hiroshi Shimada,[1] and Akinori Jyo[1]

[1]*Department of Applied Chemistry and Biochemistry, Graduate School of Science and Technology, Kumamoto University, Kumamoto, Japan*
[2]*PRESTO, Japan Science and Technology Agency, Saitama, Japan*

□ *The flexible polypyridine ligand, 2,2′:6′,2″-terpyridine (terpy), was built into the backbone of oligonucleotides to form DNA conjugates. The terpy unit functioned as a good loop when the conjugates formed the bimolecular triplexes with complementary oligopurine. The triplex structure was destabilized by the specific interaction with divalent transition metal ions (Cu^{2+}, Zn^{2+}, and Fe^{2+}), in particular Cu^{2+} ions. This ion destabilized one of the triplexes by 4.2 kcalmol^{-1} or made the triplex formation constant less than 1/10^3 at 298 K. This result is attributed to the substantial turbulence of the terminal structure of the triplexes.*

Keywords DNA triplex; terpyridine; metal ion; UV melting; amidite reagent

INTRODUCTION

Nucleic acids are the only materials that enable us to design and synthesize, from scratch, the molecules that bind given nucleic acids according to the rule of Watson-Crick base pairing.[1,2] In addition, the developing techniques of in vitro evolution have extended the target molecules to non-nucleosides.[3,4] Therefore, nucleic acids would be a versatile scaffold to construct molecular devices for analyzing not only nucleic acids,[5–8,24] but also other varieties of species in aqueous solution, such as metal ions,[9–13] proteins,[14–17] and other physiologically active substances.[18–24] Recently, researchers have been devoting their efforts to produce numbers of

Received 11 December 2007; accepted 22 May 2008.
The authors would like to thank Mr. Y. Isobe and Mr. J. Izumi for their assistance in measuring the NMR. This work was partly supported by a Grant-in-Aid for Scientific Research from MEXT, Japan to T. I.

Address correspondence to Toshihiro Ihara, Department of Applied Chemistry and Biochemistry, Graduate School of Science and Technology, Kumamoto University, 2–39-1 Kurokami, Kumamoto 860-8555, Japan. E-mail: toshi@chem.kumamoto-u.ac.jp

molecular devices based on functional nucleic acids such as ribozymes,[19,25] DNAzymes,[6–8,10–13] and aptamers.[5,9,14–23,25] Higher-order structures are critically important for these molecules to function as they are expected. The loop is a common secondary structure and an important element to determine their three-dimensional structures.

DNA is chemically stable and easily modified with auxiliary chemical groups carrying specific features.[26,27] If chemical groups that change their conformation by certain stimuli are built into the backbone in the loop moiety of the functional DNAs, we could regulate the functions indirectly by controlling the conformational changes of the DNAs. The strategy is general in the sense that it targets the conformation rather than each particular function.

In this series of studies, we chose ligands such as bipy (2,2′-bipyridine) and terpy (2,2′:6′,2″-terpyridine) as the reversible conformational modulators.[28] When the appropriate metal ion is added as a stimulus, pyridine units convergently coordinate to the metal ion to fix the whole ligands' structures. Thus, the length and flexibility of the loop structure would be controlled by choosing appropriate metal ions to be added (Figure 1). To date, it has been reported that the DNA hairpin structure[29] and β-sheet structures of peptides[30] are controlled by specific metal ions through their interaction with the substituted terpy and pyridine unit, respectively, built into the backbone structure.

Here, we report the synthesis of the amidite reagent carrying a non-substituted plain terpy unit. The unit was built into the middle of the backbone of oligopyrimidines using an automated DNA synthesizer. The

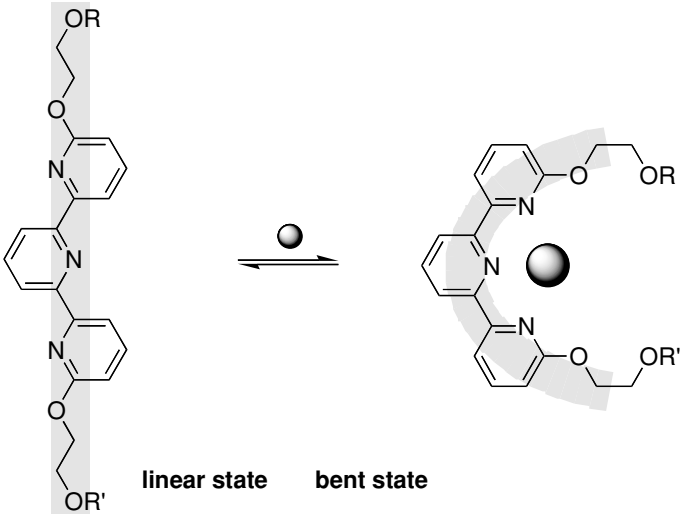

FIGURE 1 Reversible loop modification. Conformation and rigidity of the loop terpyridine unit could be controlled by complexation with metal ions.

oligopyrimidine is designed to be folded in half at the terpy position when it binds with the complementary oligopurine to form a triplex with a parallel motif.[31] The formation of the bimolecular triplexes were studied with UV melting experiments in the presence of several metal ions.

RESULTS AND DISCUSSION

Preparation of Terpy-Modified Oligopyrimidines

The 2,2′:6′,2″-terpyridine-based amidite reagent was synthesized according to Scheme 1. Generally, a diol is the key compound when one designs the synthetic scheme of an amidite reagent. One of its hydroxyl groups is tritylated by 4,4′-dimethoxytrityl chloride, and then the other is phosphitylated by chloro(diisopropylamino) (β-cyanoethoxy)phosphine to form the desired structure of the amidite reagent, which could be directly used in an automated DNA synthesizer. Here, the terpy diol (**6**) was synthesized as the key compound.

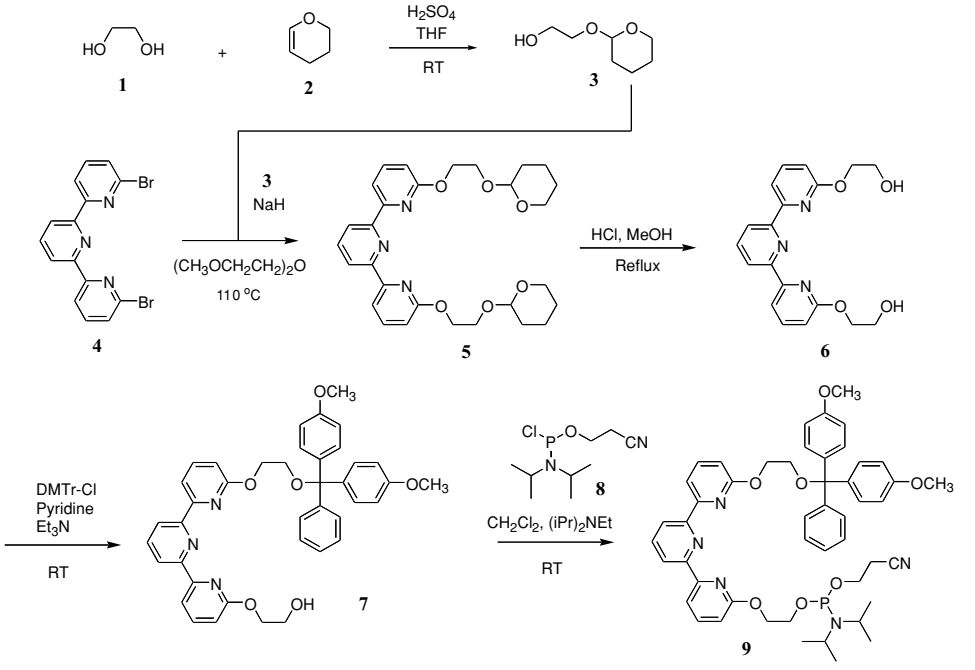

SCHEME 1 Synthesis of the terpy amidite.

One of the hydroxyl groups of ethylene glycol (**1**) was protected by 3,4-dihydro-2H-pyrane (**2**) to form 2-tetrahydropyranethanol (**3**). The **3** and 6,6″-dibromo-2,2′:6′,2″-terpyridine (**4**) was coupled by the Williamson reaction to form the protected diol **5**. This was then deprotected quantitatively in HCl-MeOH solution to afford the diol (**6**) as a white powder. Both of

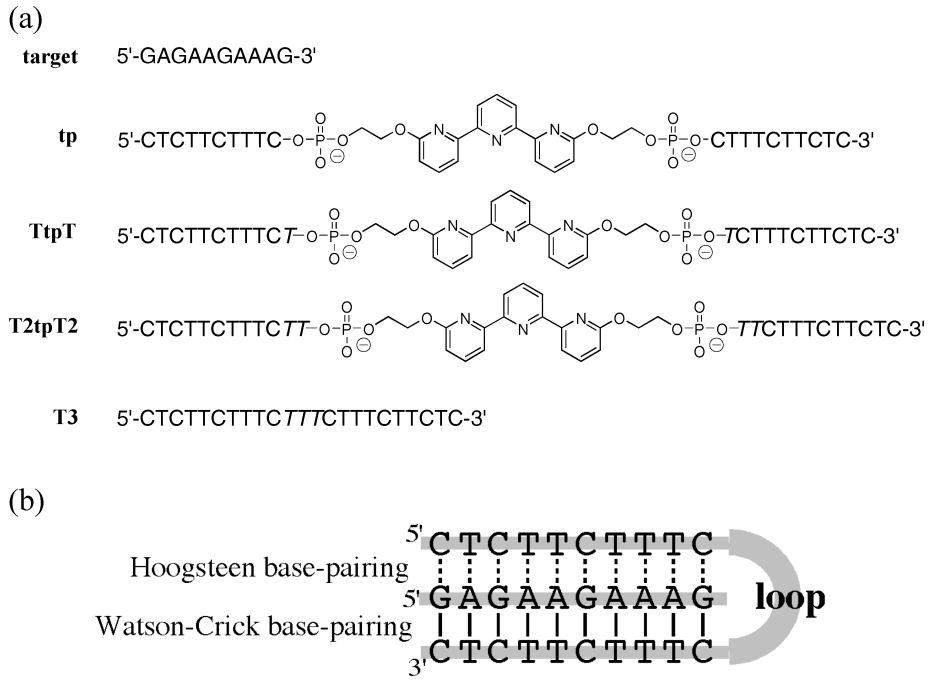

FIGURE 2 Sequences of the oligonucleotides used in this study (a) and the configuration of bimolecular triplexes (b).

the hydroxyl groups in **6** are primary ones and are supposed to have the same reactivity toward tritylation with 4,4′-dimethoxytrityl chloride. Therefore, to obtain the monotritylated alcohol (**7**) in good yield, the reaction conditions such as the feeding ratio of **6** and 4,4′-dimethoxytrityl chloride, reaction time, and temperature are critical. The crude product was chromatographed on a silica gel column with dichloromethane-diethylamine (100 : 1) to give **7** as a pale yellow powder with no decomposition during the chromatography. Finally, the amidite (**9**) was prepared by phosphitylation of **7** with chloro(diisopropy1amino)-(*β*-cyanoethoxy)phosphine (**8**). Three DNA conjugates carrying a $(dT)_n$terpy$(dT)_n$ loop (n = 0, 1, or 2 for **tp**, **TtpT**, or **T2tpT2**, respectively) were synthesized using this amidite, **9**, with the automated DNA synthesizer (Figure 2). All oligonucleotides were purified with the conventional two-step procedure using RP-HPLC (reversed-phase HPLC, linear gradient: 0.1 M triethylammonium acetate (TEAA), pH7.0/acetonitrile) and identified with MALDI-TOF mass spectrometry.[27]

Metal-Ion Effect on the Stabilities of Bimolecular Triplexes

The effect of coexisting metal ions (Cu^{2+}, Fe^{2+}, and Zn^{2+}) on the bimolecular triple helix formation was studied using UV melting experiments.

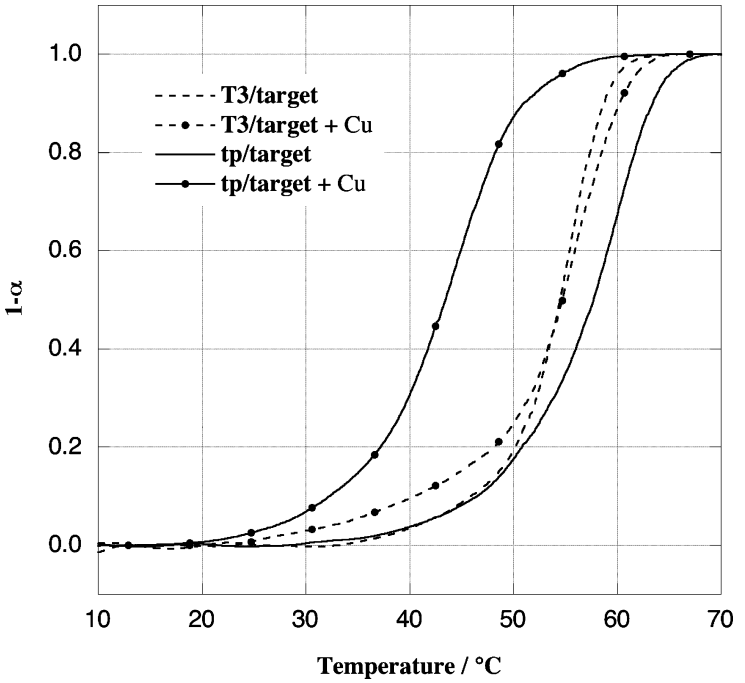

FIGURE 3 Normalized UV melting curves of the bimolecular triplexes. The solutions containing the triplexes (pH 5.0) were heated at a rate of 0.5 deg min^{-1} in the absence (without dot) and presence of Cu^{2+} (with dot). Solid curves: melting of **tp/target** triplex; broken curves: melting of **T3/target** control triplex.

All the triple helixes melted cooperatively at once. The UV melting curves for the **T3/target** and **tp/target** in the presence and absence of Cu^{2+} are shown in Figure 3. The maximum temperatures of the first derivative of the curves, T_{max}, are summarized in Table 1 and used as indicators of the triplex stabilities. The triplex of oligopyrimidines of the conjugates carrying a $(dT)_n$terpy$(dT)_n$ loop (**tp/target**, **TtpT/target**, and **T2tpT2/target**) provided higher T_{max} than that of the control $(dT)_3$ loop (**T3/target**). The $(dT)_n$terpy$(dT)_n$ loop seems to function as an excellent loop when forming the bimolecular triplexes, as compared with $(dT)_3$, probably due to the stacking interaction with the terminal base triplet ($CG.C^+$) and their appropriate length and flexibility.

Although the divalent transition metal ions scarcely change the T_{max} of the control triplex (**T3/target**), they significantly decreased the T_{max} of the triplexes containing a terpy loop (**tp/target**, **TtpT/target**, and **T2tpT2/target**). The order of the influence on the thermal stabilities of the triplexes was $Cu^{2+} > Zn^{2+} > Fe^{2+}$. This order coincides with the order of magnitude of stability constants between the terpy ligand and these metal ions.[32] Therefore, the metal ions seem to destabilize the triplex structures by their complexation with the terpy unit. The effect was already significant

TABLE 1 The T_{max} of bimolecular triplex formation in the presence and absence of three transition metal ions[a]

Pyrimidine strands	$T_{max}/°C$ $\Delta T_{max}/°C$[b]									
		$[Cu^{2+}]/\mu M$			$[Zn^{2+}]/\mu M$			$[Fe^{2+}]/\mu M$		
	No metal	1	5	10	1	5	10	1	5	10
T3	54.3	54.2	54.9	54.7	54.0	54.2	54.9	53.8	54.6	55.3
		−0.1	*0.6*	*0.4*	*−0.3*	*−0.1*	*0.6*	*−0.5*	*0.3*	*1.0*
tp	58.1	—	—	44.0	—	—	52.0	—	—	56.4
				−14.1			*−6.1*			*−1.7*
TtpT	58.2	49.3	48.3	47.5	53.3	52.8	51.8	55.7	55.5	54.5
		−8.9	*−9.9*	*−10.7*	*−4.9*	*−5.4*	*−6.4*	*−2.5*	*−2.7*	*−3.7*
T2tpT2	59.9	—	—	51.2	—	—	56.3	—	—	58.2
				−8.7			*−3.6*			*−1.7*

[a] T_{max} is defined as the temperature that provides the maximum of the 1st derivative $((dA/dT)_{max})$ of the melting curve.

[b] The values of the lower row in each cell indicated in italics are the differentials with T_{max} of "no metal".

— : not measured.

with the equimolar ratio of metal ions to the terpy units, it then became somewhat more remarkable when 5 and 10 equivalents of the ions were added. The metal ions would bind selectively to the terpy loop of the conjugates and change the conformation and flexibility of the loop. The thermodynamic parameters of triplex formation were estimated by fitting the melting curves shown in Figure 3 to the theoretical equation, which is derived based on the two state model.[33] The parameters are summarized in Table 2. Ten equivalents (10 μM) of Cu^{2+} decreased the free energy of the triplex formation by 4.2 kcalmol^{-1} at 298 K, which corresponds to a decrease of the binding constant to less than $1/10^3$. The distance between the two phosphates at both ends of the **tp** loop is ca. 21.6 Å in all of its *trans* conformations, which is almost the same with the diameter of DNA triplex. Therefore, the **tp** loop would cap one of the ends of the triplex by bridging both pyrimidine strands that was proportional to its length. That is, three pyridine rings would stack well on the terminal CG.C$^+$ to form a stable hairpin-turn structure in the absence of the metal ions. When it binds

TABLE 2 Thermodynamic parameters of the **tp**/**target** triplex formation

	$\Delta H°$/kcal mol^{-1}	$\Delta S°$/cal mol^{-1}K^{-1}	$\Delta G°_{298}$/kcal mol^{-1}	K_{298}/ M^{-1}
tp/**target**	−84.1	−226	−16.8	2.05×10^{12}
tp/**target** + 10 Cu^{2+}	−70.0	−192	−12.6	1.85×10^{9}

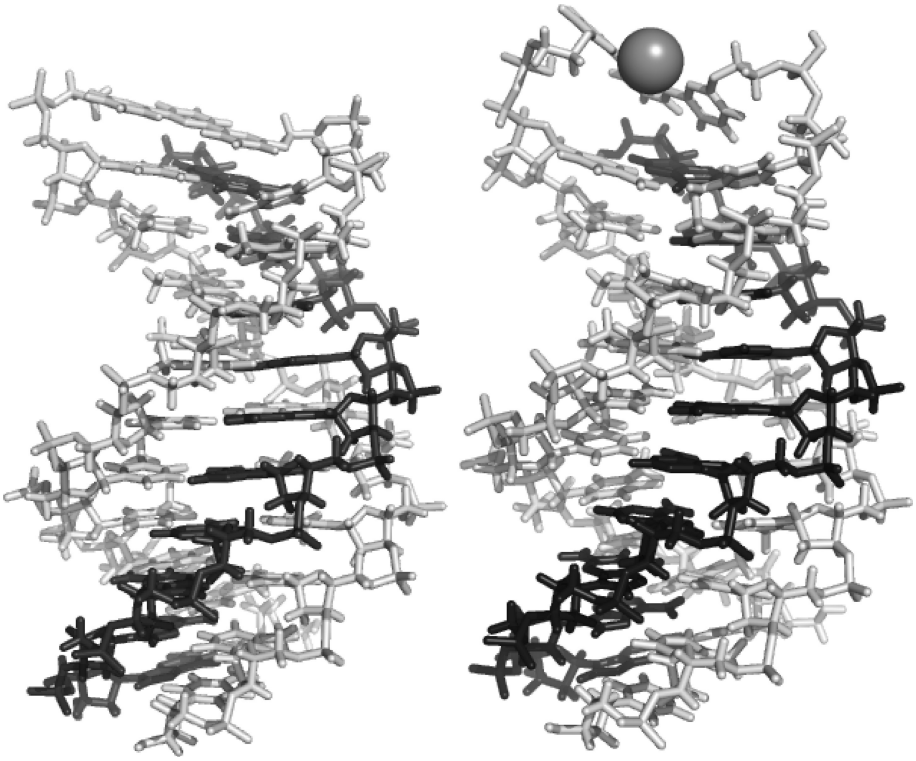

FIGURE 4 One of the possible structures of the bimolecular triplexes carrying terpy loop, **tp**/**target**, in the absence (left) and presence (right) of metal ions. White and black strands shows **tp** and **target**, respectively. The structures were optimized with an AMBER* force field using Macromodel (ver. 9.5, Schrödinger Inc.).

the metal ions, the pyridine rings flip over and direct three nitrogen atoms convergently to make space to accommodate the ions. This would make the terpy structure shorter and more rigid; the distance between the α-oxygens would be changed from ca. 12.2 to 7.4 Å by forming the complex. The possible structures of the **tp** triplex before and after complexation, which are optimized by AMBER*, are shown in Figure 4. While the free terpy stacks well on adjacent bases before complexation, an apparent perturbation of the stacking is found in the structure after complexation. The substantial destabilization of the triplexes by Cu^{2+} would be attributed to such a turbulence of the terminal structure of the triplex. The destabilization effect by the transition metal ions seemed to decrease with elongation of the loop length. This is because the strain or distortion induced by the metal complexation would be alleviated more by longer flexible loops.

CONCLUSIONS

The terpy structure was built into the backbone of oligopyrimidines to form the conjugates, **tp**, **TtpT**, and **T2tpT2**. The terpy unit functioned

as an excellent loop when the conjugates formed the triplexes with complementary oligopurine, **target**. The triplex structure was destabilized by the specific interaction with divalent transition metal ions. Among them, the effect of Cu^{2+} was most significant especially for **tp**; Cu^{2+} destabilized the **tp**/**target** triplex by 4.2 kcalmol^{-1} or made the binding constant less than $1/10^3$ at 298 K. This technique could be applied for the controlled release of DNA or RNA drugs. The loop would also be applicable as a modulator of functional nucleic acids such as ribozymes, DNAzymes, and aptamers.

EXPERIMENTAL

General

400 MHz ^{1}H and 100 MHz ^{13}C NMR spectra were measured on a EX400 spectrometer (JEOL, Japan) at 298 K. ^{31}P NMR spectrum was measured on a Unity Inova 400 (Brucker, Germany). Chemical shifts (δ) are expressed in ppm relative to $SiMe_4$ for ^{1}H and ^{13}C, and phosphate for ^{31}P-NMR. Multiplicities are indicated as the following: s (singlet); d (doublet); dd (double doublets); dt (double triplets); t (triplet); m (multiplet). ^{1}H NMR coupling constants (J) are reported in Hz. IR spectra were collected on an FTIR Spectrum one spectrometer (Perkin Elmer, USA). Elemental analysis was performed on a CHN Corder MT-6 (Yanaco, Japan). Matrix-assisted laser desorption ionization mass spectrometry measurements (MALDI-TOF/MS) were carried out using a Voyager RP mass spectrometer (PerSeptive, USA). Electrospray ionization-time of flight mass spectrometry (ESI-TOF/MS) measurements of terpy amidite was carried out using a solution of acetonitrile saturated with lithium chloride with a LCT spectrometer (Micromass, UK) in positive ion mode.[34]

Synthesis of Terpy Amidite (9)

Protected diol (3): Ethylene glycol (**1**) (0.45 mL, 8.1 mmol) and 3,4-dihydro-2H-pyrane (**2**) (0.88 mL, 9.7 mmol) were dissolved in 5 mL of THF under an atmosphere of argon. Sulfuric acid (0.012 mL) was added to the mixture and the mixture was stirred for 2 hours at room temperature. The mixture was diluted with 10 mL of ethyl acetate and washed with 5 mL of brine and saturated sodium hydrogen carbonate. The organic phase was separated, dried with anhydrous $MgSO_4$, and concentrated to dryness under reduced pressure. The residue was subjected to silica gel column chromatography (hexane : ethyl acetate = 4 : 1) and the fraction of R_f 0.25 was collected. The fraction was concentrated to dryness in vacuo to afford a light yellow liquid.

Yield 0.59 g (50%); yellow liquid; ^{1}H-NMR ($CDCl_3$) δ 4.58 (1H, m, O-CH-O), 3.90–4.00, 3.65–3.80, 3.50–3.60 (1H, 4H, 1H, m, O-CH_2), 3.02 (1H, s, OH), 1.72–1.90, 1.50–1.63 (2H, 4H, m, C-CH_2-C).

Protected terpy diol (5):[35] Sodium hydride (60 mg, 1.5 mmol) was suspended in 3 mL dry diglyme (bis(2-methoxyethyl) ether) under an atmosphere of argon. Tetrahydropyran ethanol (**3**) (0.21 mL, 1.5 mmol) was added slowly to the solution in an ice bath. After the termination of gas generation, dibromoterpyridine (**4**) (0.1 g, 0.26 mmol) was added into the solution and stirred at 110°C for 12 hours. Analysis by RP-TLC indicated the presence of a new component (R_f 0.2, acetonitrile : water = 6 : 1) and the disappearance of **8**. After standing to cool, the resulting white precipitate was filtered. The filtrate was diluted with ethyl acetate and washed twice with water. The organic phase was separated, dried with anhydrous $MgSO_4$, and concentrated to dryness under reduced pressure. Recrystallization from 1-butanol afforded **5** as white crystals.

Yield 92 mg (69%); white crystals, m.p. 107–108°C; ^{1}H NMR ($CDCl_3$) δ 8.30 (2H, d, J = 7.81, Ar-5,5″H), 8.14 (2H, d, J = 7.81, Ar-3,3″H), 7.82 (1H, t, J = 7.71, Ar-4′H), 7.66 (2H, t, J = 7.81, Ar-4,4″H), 6.76 (2H, d, J = 8.30, Ar-3′,5′H), 4.60, 4.06, 3.83, 3.45 (14H, m, OCH_2, THP-2,2′,6,6′H) 1.62 (12H, m, THP-3,4,5,3′,4′,5′H); ^{13}C NMR ($CDCl_3$) δ 180.8 (C), 172.8 (C), 171.7 (C), 157.1 (CH), 155.3 (CH), 138.4 (CH), 131.6 (CH), 129.2 (CH), 116.6 (CH) and 83.5 (CH_2) 82.6 (CH_2) 79.9 (CH_2) 48.3 (CH_2) 43.1 (CH_2) 37.1 (CH_2); IR (KBr) ν 3448, 2945, 1742, 1601, 1572, 1470, 1380, 1322, 1337, 1265, 1235, 1201, 1184, 1143, 1128, 1076, 1937, 1024, 991, 944, 930, 907, 889, 874, 815, 794, 763, 747, 632 cm^{-1}; Anal. Calcd for $C_{29}H_{35}N_3O_6$: C 66.78, H 6.76, N 8.06%, Found: C 66.75, H 6.65, N 8.25%.

Terpy diol (6): Protected terpy diol (0.24 g, 0.47 mmol) was dissolved in 10 mL HCl-CH_3OH (1 : 4) and the solution was refluxed for 1 hour. After standing to cool, the solution was basified by potassium carbonate. The resulting white precipitate was collected and washed with water. The product was used for the next step synthesis without further purification, because an NMR study showed that the purity was more than 99%.

Yield 0.16 g (95%); white crystals, m.p. 203.8–204.0°C; ^{1}H NMR (DMSO-d_6) δ 8.37 (2H, d, J = 7.81, Ar-5,5″H), 8.19 (2H, d, J = 7.32, Ar-3,3″H), 8.09 (1H, t, J = 7.81, Ar-4′), 7.90 (2H, t, J = 7.81, Ar-4,4″), 6.92 (2H, d, J = 8.30, Ar-5′,3′H), 4.90 (2H, t, J = 5.37, OH), 4,46 (4H, t, J = 5.37, Ar-OCH_2), 3.81 (4H, t, J = 5.37, CH_2-OH); ^{13}C NMR (DMSO) δ 162.9 (C) 154.5 (C), 152.6 (C), 140.2 (CH), 138.4 (CH), 120.5 (CH), 113.6 (CH), 111.4 (CH), 67.3 (CH_2), 59.4 (CH_2); IR (KBr) ν 3327, 2953, 1603, 1572, 1471, 1438, 1380, 1339, 1323, 1272, 1074, 1047, 991, 943, 888, 792, 735, 634 cm^{-1}; Anal. Calcd for $C_{19}H_{19}N_3O_4$: C 64.58, H 5.42, N 11.89%, Found: C 64.54, H 5.49, N 11.80%; MALDI-TOF/MS (CHCA matrix) Calcd: 354.14, Found: 352.76.

Monotrityl terpy (7):[28] Terpy diol (**6**) (0.10 g, 0.28 mmol) was added into 4 mL of anhydrous pyridine under an atmosphere of argon. To the suspension, triethylamine (0.07 mL, 0.51 mmol) and 4,4′-dimethoxytrityl chloride (96 mg, 0.28 mmol) were added and then the suspension was stirred for 2 hours at 25°C. The reaction was quenched by addition of methanol (1 mL). The reaction mixture was diluted with 10 mL of dichloromethane and then washed twice with 5% aqueous NaOH (50 mL). The organic phase was dried with anhydrous $MgSO_4$ and concentrated in vacuo. The residue was subjected to silica gel column chromatography. The column was packed with the silica slurry suspended in the solution of dichloromethane-diethylamine (100 : 5) and then washed with dichloromethane of three bed volumes. Separation was carried out with hexane-ethyl acetate (3 : 2), and the fraction of R_f 0.24 was collected. It was concentrated to dryness in vacuo to give pale yellow crystals. The product was used for the next step synthesis without further purification, because an NMR study showed that the purity was more than 99%.

Yield 0.114 g (30%); yellow powder; ^{1}H-NMR ($CDCl_3$) δ 8.43 (1H, d, J = 7.79, Ar-5″H), 8.28 (1H, d, J = 6.83, Ar-5H), 8.22 (2H, dd, J = 4.88, 5.87, Ar-3,3″H), 7.89 (1H, t, J = 7.83, Ar-4′H), 7.76 (2H, dt, J = 6.35, 7.79, Ar-4,4″H), 7.51–7.17 (9H, m, DMTr), 6.86–6.79 (6H, m, DMTr, Ar-3′,5′H), 4.68 (2H, t, J = 4.87, Ar-OCH_2), 4.63 (2H, t, J = 4.87, Ar-OCH_2), 4.04 (2H, t, J = 4.87, CH_2-OH), 3.76 (6H, s, OCH_3), 3.49 (2H, t, J = 4.87, CH_2-O-DMTr); ^{13}C NMR (DMSO-d_6) δ 163.3 (C), 148.4 (C), 155.4 (C), 154.7 (C), 153.6 (C), 153.3 (C), 145.0 (C), 139.8 (CH), 139.4 (CH), 137.7 (CH), 136.3 (CH), 130.1 (CH), 128.2 (CH), 127.7 (CH), 126.7 (CH), 120.9 (CH), 120.5 (CH), 114.4 (CH), 113.9 (CH), 113.0 (CH), 111.5 (CH), 85.9 (CH), 68.2 (CH_2), 65.0 (CH_2), 62.5 (CH_2), 62.4 (CH_2), 55.2 (CH).

Terpy amidite (9): Monotrityl terpy (**7**) (95 mg, 0.15 mmol) was dissolved in 3 mL of anhydrous dichloromethane under an atmosphere of argon. To the solution, diisopropylethylamine (0.21 mL, 1.22 mmol) and chloro(diisopropylamino)-(β-cyanoethoxy)phosphine (**8**) (0.068 mL, 0.30 mmol) was added and the solution was stirred for 1 hour at 25°C. Analysis by TLC (dichloromethane : ethyl acetate = 2 : 1, 1% triethylamine) indicated the presence of a new component (R_f 0.90) and the disappearance of **7** (R_f 0.30). The reaction mixture was diluted with 5 mL of dichloromethane, washed twice with 5% aqueous $NaHCO_3$ (10 mL), dried with anhydrous $MgSO_4$, and concentrated in vacuo. The residue was purified by chromatography on silica gel (dichloromethane : ethyl acetate : triethylamine = 100 : 50 : 1). The component of R_f 0.9 was collected and concentrated to dryness in vacuo.

Yield 35 mg (24%); white powder; ^{1}H-NMR ($CDCl_3$) δ 8.29 (1H, d, J = 7.79, Ar-5″H), 8.24 (1H, d, J = 7.79, Ar-5H), 8.14 (2H, dd, Ar-3,3″H), 7.80 (1H, t, J = 7.83, Ar-4′H), 7.66 (2H, dt, Ar-4,4″H), 7.43–7.11 (9H, m, DMTr),

6.77–6.71 (6H, m, DMTr, Ar-3′,5′H), 4.59 (4H, m, Ar-OCH_2), 4.04 (2H, m, CH_2-O-P), 3.78, 3.57 (4H, m, N-CH, P-OCH_2), 3.69 (6H, s, Ar-OCH_3), 3.42 (2H, t, $J = 4.87$, CH_2-O-DMTr), 2.55 (2H, t, $J = 4.87$, CH_2-CN), 1.18 (12H, m, $(iPr)_2$); ^{13}C NMR ($CDCl_3$) δ 163.1, 158.4, 153.54, 145.1, 139.5, 139.4, 137.5, 136.3, 130.1, 128.3, 127.8, 126.7, 120.7, 120.6, 114.0, 113.8, 113.1, 111.4, 86.0, 65.5, 65.0, 62.4, 62.1, 60.4, 58.7, 58.5, 55.2, 53.4, 43.2, 43.1 29.7, 24.6, 20.4, 20.3; ^{31}P-NMR ($CDCl_3$) δ 147.16; ESI-TOF/MS for $C_{49}H_{54}N_5O_7P$ (mixed with saturated LiCl solution) Calcd: 862.39 $[M+Li]^+$, Found: 862.62.

Oligonucleotides: All oligonucleotides (ODNs) used in this study were purchased from Hokkaido System Science Co., Ltd. (Japan), or synthesized using Expedite 8900 (Applied Biosystems, USA) DNA synthesizer with dimethoxytrityl phosphoramidite reagents purchased from Glen Research (USA) or Proligo (Germany). All other reagents were purchased and used without further purification. The synthesis followed the regular protocol for the DNA synthesizer except for the cycle of terpy amidite (**9**), in which prolonged coupling time of 10 minutes and capping time of 15 minutes were used. The ODNs or ODN conjugates were purified from the crude mixture by RP-HPLC (reversed phase-HPLC, LC-2000plus inert system, Jasco) equipped with an ODS column (Wakopak-Wakosil-II 5C18 RS, 4.6 mm (φ) × 150 mm (w), Wako, Japan). MALDI-TOF/MS measurements of ODNs and ODN conjugates were measured in negative ion mode with 3-hydroxypicolinic acid as a matrix. The concentration of the ODN solution was determined at 25°C based on the molar extinction coefficients calculated using those of nearest-neighbor dinucleoside monophosphates at 260 nm obtained from the literature.[36]

MALDI-TOF/MS (3-HPA matrix) for **tp** Calcd: 6315.13, Found: 6316.25; for **TtpT** Calcd: 6921.15, Found: 6921.24; for **T2tpT2** Calcd: 7529.24, Found: 7531.20

UV Melting[37]

Thermal denaturation experiments were carried out in sodium acetate buffer solution (100 mM, pH 5.0) containing 10 mM NaCl and 10 mM $MgCl_2$ on a V-560 (Jasco, Japan) or UV-1650 (Shimadzu, Japan) UV/Vis spectrophotometer equipped with a Peltier thermal controller. Concentrations of each component of the triplexes (**target**, **tp**, **TtpT**, and **T2tpT2**) were 1 μM. Prior to the beginning of each melt, the samples were degassed at 85°C for 5 minutes and then annealed with slow cooling to 0°C. In the denaturation experiments, the solutions were heated at a rate of 0.5 deg min^{-1} after equilibration for 20 minutes at 0°C.

The thermodynamic parameters of the triplex formation were estimated by fitting the experimental curves to the theoretical one, which is derived

assuming the two-state model, using the Levenberg-Marquardt nonlinear least-squares method.[33]

Molecular Modeling

The molecular models were constructed with Macromodel (ver. 9.5, Schrödinger Inc., USA). The initial structure was built as a standard double helix using the Maestro (Schrödinger, Inc.) fragment library. The simulations were carried out with an AMBER* force field with GB/SA treatment of solvation.

REFERENCES

1. Storhoff, J.J.; Mirkin, C.A. Programmed materials synthesis with DNA. *Chem. Rev.* **1999**, 99, 1849–1862.
2. Bath. J.; Turberfield, A.J. DNA nanomachine. *Nat. Nanotechnol.* **2007**, 2, 275–284.
3. Joyce, G.F. Forty years of in vitro evolution. *Angew. Chem. Int. Ed.* **2007**, 46, 6420–6436.
4. Famulok, M. Oligonucleotide aptamers that recognize small molecules. *Curr. Opin. Struct. Biol.* **1999**, 9, 324–329.
5. Kolpashchikov, D.M. Binary malachite green aptamer for fluorescent detection of nucleic acids. *J. Am. Chem. Soc.* **2005**, 127, 12442–12443.
6. Tian, Y.; Mao, C. DNAzyme amplification of molecular beacon signal. *Talanta* **2005**, 67, 532–537. DNA
7. Niazov, T.; Pavlov, V.; Xiao, Y.; Gill, R.; Willner, I. DNAzyme-functionalized Au nanoparticles for the amplified detection of DNA or telomerase activity. *Nano Lett.* **2004**, 4, 1683–1687.
8. Sando, S.; Sasaki, T.; Kanatani, K.; Aoyama, Y. Amplified nucleic acid sensing using programmed self-cleaving DNAzyme. *J. Am. Chem. Soc.* **2003**, 125, 15720–15721.
9. Wang, L.; Liu, X.; Hu, X.; Song, S.; Fan, C. Unmodified gold nanoparticles as a colorimetric probe for potassium DNA aptamer. *Chem. Commun.* **2006**, 3780–3782.
10. Liu, J.; Lu, Y. Rational design of "turn-on" allosteric DNAzyme catalytic beacons for aqueous mercury ions with ultrahigh sensitivity and selectivity. *Angew. Chem. Int. Ed.* **2007**, 46, 7587–7590.
11. Liu, J.; Lu, Y. Accelerated color change of gold nanoparticles assembled by DNAzymes for simple and fast colorimetric Pb^{2+} detection. *J. Am. Chem. Soc.* **2004**, 126, 12298–12305.
12. Liu, J.; Lu, Y. A DNAzyme catalytic beacon sensor for paramagnetic Cu^{2+} ions in aqueous solution with high sensitivity and selectivity. *J. Am. Chem. Soc.* **2007**, 129, 9838–9839.
13. Xiao, Y.; Rowe, A.A.; Plaxco, K.W. Electrochemical detection of parts-per billion lead via an electrode-bound DNAzyme assembly. *J. Am. Chem. Soc.* **2007**, 129, 262–263.
14. Y.-Fujita, R.; Kumar, P.K.R. Aptamer-derived nucleic acid oligos: Applications to develop nucleic acid chips to analyze proteins and small ligands. *Anal. Chem.* **2005**, 77, 5460–5466.
15. Xiao, Y.; Piorek, B.D.; Plaxco, K.W.; Heeger, A.J. A reagentless signal-on architecture for electronic, aptamer-based sensors via target-induced strand displacement. *J. Am. Chem. Soc.* **2005**, 127, 17990–17991.
16. Zhou, L.; Ou, L.-J.; Chu, X.; Shen, G.-L.; Yu, R.-Q. Aptamer-based rolling circle amplification: A platform for electrochemical detection of protein. *Anal. Chem.* **2007**, 79, 7492–7500.
17. Smith, J.E.; Medley, C.D.; Tang, Z.; Shangguan, D.; Lofton, C.; Tan, W. Aptamer-conjugated nanoparticles for the collection and detection of multiple cancer cells. *Anal. Chem.* **2007**, 79, 3075–3082.
18. Rupcich, N.; Nutiu, R.; Li, Y.; Brennan, J.D. Entrapment of fluorescent signaling DNA aptamers in sol-gel-derived silica. *Anal. Chem.* **2005**, 77, 4300–4307.
19. Brackett, D.M.; Dieckmann, T. Aptamer to ribozyme: The intrinsic catalytic potential of a small RNA. *Chem. Bio. Chem.* **2006**, 7, 839–843.
20. Sparano, B.A.; Koide, K. A strategy for the development of small-molecule-based sensors that strongly fluoresce when bound to a specific RNA. *J. Am. Chem. Soc.* **2005**, 127, 14954–14955.

21. Shen, L.; Chen, Z.; Li, Y.; Jing, P.; Xie, S.; He, S.; He, P.; Shao, Y. A chronocoulometric aptamer sensor for adenosine monophosphate. *Chem. Commun.* **2007**, 2169–2171.
22. Zayats, M.; Huang, Y.; Gill, R.; Ma, C.; Willner, I. Label-free and reagentless aptamer-based sensors for small molecules. *J. Am. Chem. Soc.* **2006**, 128, 13666–13667.
23. Liu, J.; Lu, Y. Non-base pairing DNA provides a new dimension for controlling aptamer-linked nanoparticles and sensors. *J. Am. Chem. Soc.* **2007**, 129, 8634–8643.
24. Micura, R. Programmable ligand-controlled riboregulators. *Angew. Chem. Int. Ed.* **2006**, 45, 30–31.
25. Famulok, M.; Hartig, J.S.; Mayer, G. Functional aptamers and aptazymes in biotechnology, diagnostics, and therapy. *Chem. Rev.* **2007**, 107, 3715–3743.
26. Hermanson, G.T. *Bioconjugate techniques*. Academic Press: San Diego, 1996.
27. Agrawal, S. (Ed.) *Methods in Molecular Biology, Protocols for Oligonucleotide Conjugates, Synthesis and Analytical Techniques*. Humana Press: Totowa, 1994.
28. Ihara, T.; Shirasaka, Y.; Sato, Y.; Kitamura, Y.; Okada, K.; Tazaki, M.; Jyo, A. Synthesis of the amidite reagent to built bipyridine units into DNA backbone. *Heterocycles* **2005**, 65, 293–301.
29. Bianké, G.; Häner, R. A metal-coordinating DNA hairpin mimic. *ChemBioChem* **2004**, 5, 1063–1068.
30. Schneider, J.P.; Kelly, J.W. Synthesis and efficacy of square planar copper complexes designed to nucleate β-sheet structure. *J. Am. Chem. Soc.* **1995**, 117, 2533–2546.
31. Xodo, L.E.; Manzini, G.; Quadrifoglio, F. Spectroscopic and calorimetric investigation on the DNA triple helix formed by d(CTCTTCTTTCTTTTCTTTCTTCTC) and d(GAGAAGAAAGA) at acidic pH. *Nucleic Acids Res.* **1990**, 18, 3557–3564.
32. Sillén, L.G.; Martell, A.E. *Stability constants of metal-ion complexes*. The Chemical Society: London, 1964.
33. Marky, L.A.; Breslauer, K.J. Calculating thermodynamic data for transitions of any molecularity from equilibrium melting curve. *Biopolymers* **1987**, 26, 1601–1620.
34. Kupihár, Z.; Timár, Z.; Dellinger, D.J.; Caruthers, M.H. Accurate mass analysis of phosphoramidites by electrospray mass spectrometry. *Nucleos. Nucleot. Nucl.* **2004**, 23, 767–775.
35. Newkome, G.R.; Nayak, A.; McClure, G.L.; Danesh-Khoshboo, F.; Broussard-Simpson, J. Chemistry of heterocyclic compounds. 23. Synthesis of multiheteromacrocycles possessing 2,6-pyridino subunits connected by carbon-oxygen linkages. *J. Org. Chem.* **1977**, 42, 1500–1508.
36. Cantor, C.R.; Warshaw, M.M. Oligonucleotide interactions. III. Circular dichroism studies of the conformation of deoxyoligonucleotides. *Biopolymers* **1970**, 9, 1059–1077.
37. Ihara, T.; Takeda, Y.; Jyo, A. Metal ion-directed cooperative triple helix formation of glutamic acid-oligonucleotide conjugate. *J. Am. Chem. Soc.* **2001**, 123, 1772–1773.